THE UNIVERSITY OF WARWICK

Original citation:
LHCb Collaboration (Including: Back, J. J., Blake, Thomas, Craik, Daniel, Dossett, D., Gershon, T. J., Kreps, Michal, Latham, Thomas, Pilar, T., Poluektov, Anton, Reid, Matthew M., Silva Coutinho, R., Wallace, Charlotte, Whitehead, M. (Mark) and Williams, M. P.). (2014) Evidence for the decay $B+c \rightarrow J/\psi 3\pi + 2\pi-$. Journal of High Energy Physics, Volume 2014 (Number 5). Article number 148.

Permanent WRAP url:
http://wrap.warwick.ac.uk/62850

A note on versions:
The version presented in WRAP is the published version, or, version of record, and may be cited as it appears here.

For more information, please contact the WRAP Team at: publications@warwick.ac.uk

warwickpublicationswrap

highlight your research

http://wrap.warwick.ac.uk

Evidence for the decay $B_c^+ \rightarrow J/\psi\, 3\pi^+ 2\pi^-$

The LHCb collaboration

E-mail: Ivan.Belyaev@cern.ch

ABSTRACT: Evidence is presented for the decay $B_c^+ \rightarrow J/\psi\, 3\pi^+ 2\pi^-$ using proton-proton collision data, corresponding to an integrated luminosity of $3\,\text{fb}^{-1}$, collected with the LHCb detector. A signal yield of 32 ± 8 decays is found with a significance of 4.5 standard deviations. The ratio of the branching fraction of the $B_c^+ \rightarrow J/\psi\, 3\pi^+ 2\pi^-$ decay to that of the $B_c^+ \rightarrow J/\psi\, \pi^+$ decay is measured to be

$$\frac{\mathcal{B}\left(B_c^+ \rightarrow J/\psi\, 3\pi^+ 2\pi^-\right)}{\mathcal{B}\left(B_c^+ \rightarrow J/\psi\, \pi^+\right)} = 1.74 \pm 0.44 \pm 0.24,$$

where the first uncertainty is statistical and the second is systematic.

KEYWORDS: Hadron-Hadron Scattering, QCD, Branching fraction, B physics, Flavor physics

Contents

1 Introduction

The B_c^+ meson is the only meson consisting of two heavy quarks of different flavours. It was discovered by the CDF collaboration through the semileptonic decay $B_c^+ \to J/\psi \, \ell^+ \nu_\ell X$ [1], where X denotes possible unobserved particles.[1] The CDF collaboration also observed the hadronic decay mode $B_c^+ \to J/\psi \, \pi^+$ [2]. Recently, the LHCb experiment has observed several new channels including $B_c^+ \to J/\psi \, \pi^+ \pi^+ \pi^-$ [3], $B_c^+ \to \psi(2S)\pi^+$ [4], $B_c^+ \to J/\psi \, D_s^+$ and $B_c^+ \to J/\psi \, D_s^{*+}$ [5], $B_c^+ \to J/\psi \, K^+$ [6], $B_c^+ \to J/\psi \, K^+ K^- \pi^+$ [7] and $B_c^+ \to B_s^0 \pi^+$ [8]. The lifetime of the B_c^+ meson [9, 10] is about three times shorter than that of the B^0 and B^+ mesons, confirming the important role played by the c quark in B_c^+ decays. The decays of B_c^+ mesons into charmonia and light hadrons are expected to be well described by the factorization approximation [11, 12]. In this scheme, the $B_c^+ \to J/\psi \, 3\pi^+ 2\pi^-$ decay is characterized by the form factors of the $B_c^+ \to J/\psi \, W^+$ transition and the spectral functions for the virtual W^+ boson into light hadrons [13]. The predictions for the ratio of branching fractions

$$R_{5\pi} \equiv \frac{\mathcal{B}\left(B_c^+ \to J/\psi \, 3\pi^+ 2\pi^-\right)}{\mathcal{B}\left(B_c^+ \to J/\psi \, \pi^+\right)} \tag{1.1}$$

are 0.95 and 1.1 [14], using form factor calculations from refs. [15] and [16], respectively.

In this article, the first evidence for the decay $B_c^+ \to J/\psi \, 3\pi^+ 2\pi^-$ and a measurement of $R_{5\pi}$ are reported. The analysis is based on a data sample of proton-proton (pp) collisions, corresponding to an integrated luminosity of $1\,\text{fb}^{-1}$ at a centre-of-mass energy of $7\,\text{TeV}$ and $2\,\text{fb}^{-1}$ at $8\,\text{TeV}$, collected with the LHCb detector.

---

[1]The inclusion of charge conjugate modes is implicit throughout this paper.

2 Detector

The LHCb detector [17] is a single-arm forward spectrometer covering the pseudorapidity range $2 < \eta < 5$, designed for the study of particles containing b or c quarks. The detector includes a high-precision tracking system consisting of a silicon-strip vertex detector surrounding the pp interaction region, a large-area silicon-strip detector located upstream of a dipole magnet with a bending power of about $4\,\mathrm{Tm}$, and three stations of silicon-strip detectors and straw drift tubes [18] placed downstream. The combined tracking system provides a momentum measurement with relative uncertainty that varies from 0.4% at $5\,\mathrm{GeV}/c$ to 0.6% at $100\,\mathrm{GeV}/c$, and impact parameter resolution of $20\,\mu\mathrm{m}$ for tracks with large transverse momentum. Different types of charged hadrons are distinguished using information from two ring-imaging Cherenkov detectors [19]. Photon, electron and hadron candidates are identified by a calorimeter system consisting of scintillating-pad and preshower detectors, an electromagnetic calorimeter and a hadronic calorimeter. Muons are identified by a system composed of alternating layers of iron and multiwire proportional chambers [20]. The trigger [21] consists of a hardware stage, based on information from the calorimeter and muon systems, followed by a software stage, which applies a full event reconstruction.

This analysis uses events collected by triggers that select the $\mu^+\mu^-$ pair from the J/ψ decay with high efficiency. At the hardware stage either one or two muon candidates are required to trigger the event. In the case of single muon triggers, the transverse momentum, p_{T}, of the muon candidate is required to be greater than $1.5\,\mathrm{GeV}/c$. For dimuon candidates, the product of the p_{T} of muon candidates is required to satisfy $\sqrt{p_{\mathrm{T}1}p_{\mathrm{T}2}} > 1.3\,\mathrm{GeV}/c$. At the subsequent software trigger stage, two muons are selected with an invariant mass in the range $2.97 < m_{\mu^+\mu^-} < 3.21\,\mathrm{GeV}/c^2$ and consistent with originating from a common vertex. The common vertex is required to be significantly displaced from the pp collision vertices.

Simulated pp collisions are generated using PYTHIA 6.4 [22] with the configuration described in ref. [23]. Final-state QED radiative corrections are included using the PHOTOS package [24]. The B_c^+ mesons are produced by a dedicated generator, BCVEGPY [25]. The decays of all hadrons are performed by EVTGEN [26], and a specific model is implemented to generate the decays $\mathrm{B}_c^+ \to \mathrm{J}/\psi\, 3\pi^+2\pi^-$, assuming factorization [14]. The model allows the implementation of different form factors for this decay, calculated using QCD sum rules [15] or a relativistic quark model [16]. These predictions lead to very similar values and those based on the relativistic quark model are used in the simulation. The coupling of the five pion $(3\pi^+2\pi^-)$ system to the virtual W^+ is taken from τ^+ lepton decays [27]. The interaction of the generated particles with the detector and its response are implemented using the GEANT4 toolkit [28, 29] as described in ref. [30].

3 Candidate selection

The decays $\mathrm{B}_c^+ \to \mathrm{J}/\psi\, 3\pi^+2\pi^-$ and $\mathrm{B}_c^+ \to \mathrm{J}/\psi\,\pi^+$ are reconstructed using the J/$\psi \to \mu^+\mu^-$ decay mode. The selection criteria chosen are similar for both channels.

All tracks are required to be in the pseudorapidity range $2 < \eta < 4.9$. Good track quality of charged particles is ensured by requiring the χ^2 per number of degrees of freedom, χ^2/ndf, provided by the track fit, to be less than 3. Suppression of fake tracks created by the reconstruction is achieved by a neural network trained with simulated samples to discriminate between fake tracks and tracks associated with real particles [31], ensuring the rate of fake tracks below $0.3\,\%$.

Two dedicated neural networks are used for muon and pion identification. These networks use the information from the Cherenkov detectors [19], muon chambers [32] and the calorimeter system [33], together with the tracking information. The momentum of the pion candidates is required to be between $3.2\,\text{GeV}/c$ and $150\,\text{GeV}/c$ in order to ensure good quality particle identification in Cherenkov detectors. The requirements on the neural network output are chosen to ensure good agreement between data and simulation and significant reduction of the background due to misidentification.

Pairs of oppositely charged muons, originating from a common vertex, are combined to form $J/\psi \to \mu^+\mu^-$ candidates. The p_{T} of each muon is required to be greater than $550\,\text{MeV}/c$. Good vertex reconstruction is ensured by requiring the χ^2 of the vertex fit, χ^2_{vtx}, to be less than 20. To select dimuon vertices that are well-separated from the reconstructed pp interaction vertices, the decay length is required to be at least three times its uncertainty. The invariant mass of the dimuon combination is required to be between 3.020 and $3.135\,\text{GeV}/c^2$. The asymmetric mass range with respect to the known J/ψ meson mass [9] is chosen to include the QED radiative tail.

The selected J/ψ candidates are combined with pions to form $B_c^+ \to J/\psi\,3\pi^+2\pi^-$ and $B_c^+ \to J/\psi\,\pi^+$ candidates. The transverse momentum of each pion is required to be greater than $400\,\text{MeV}/c$. To ensure that the pions are inconsistent with being directly produced in a pp interaction, the impact parameter χ^2, defined as the difference between the χ^2 values of the fits of the pp collision vertex formed with and without the considered pion track, is required to satisfy $\chi^2_{\text{IP}} > 4$. When more than one primary vertex is reconstructed, the vertex with the smallest value of χ^2_{IP} is chosen. Good vertex reconstruction for the B_c^+ candidate vertex is ensured by requiring the $\chi^2_{\text{vtx}}/\text{ndf}$ to be less than 12. To suppress the large combinatorial background in the $B_c^+ \to J/\psi\,3\pi^+2\pi^-$ sample, the χ^2 of the vertex fit for all $J/\psi\,\pi^\pm$ combinations, as well as for all dipion combinations, is required to be less than 20. To improve the invariant mass resolution, a kinematic fit [34] is performed that constrains the $\mu^+\mu^-$ pair to the known mass of the J/ψ meson. It is also required that the B_c^+ candidate's momentum vector points back to from the associated pp interaction vertex. The χ^2 per number of degrees of freedom of the fit, $\chi^2_{\text{fit}}/\text{ndf}$, is required to be less than 5. The measured decay time of the B_c^+ candidate, calculated with respect to the associated primary vertex, is required to be between $150\,\mu\text{m}/c$ and $1\,\text{mm}/c$.

4 Signal and normalization yields

The mass distribution for the selected $J/\psi\,3\pi^+2\pi^-$ candidates is shown in figure 1. To estimate the signal yield, an extended maximum likelihood fit to the unbinned mass distribution is made. The $B_c^+ \to J/\psi\,3\pi^+2\pi^-$ signal is modelled by a Gaussian distribution

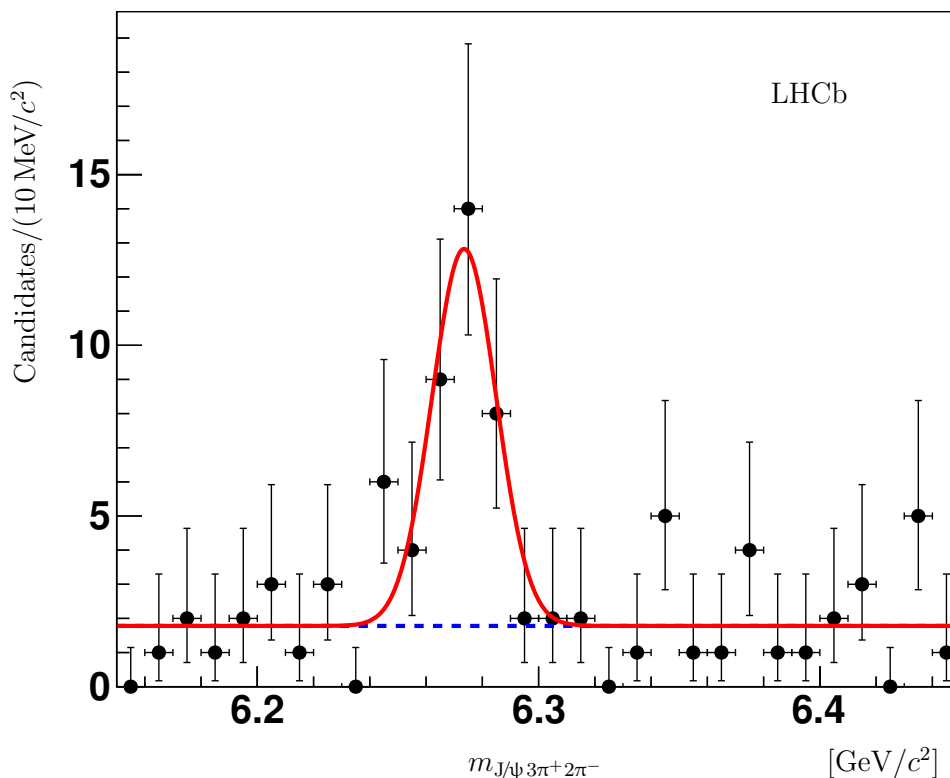**Figure 1**. Mass distribution for selected $B_c^+ \to J/\psi\, 3\pi^+ 2\pi^-$ candidates. The result of a fit using the model described in the text (red solid line) is shown together with the background component (blue dashed line).

and the background by a constant function. The fit results for the fitted mass and mass resolution of B_c^+ signal, $m_{B_c^+}$ and $\sigma_{B_c^+}$, and signal yield $N_{B_c^+ \to J/\psi\, 3\pi^+ 2\pi^-}$, are listed in table 1,

The statistical significance for the observed signal is determined as $\mathcal{S}_\sigma = \sqrt{-2\log\frac{\mathcal{L}_B}{\mathcal{L}_{S+B}}}$ where $\mathcal{L}_{S+B}$ and $\mathcal{L}_B$ denote the likelihood associated with the signal-plus-background and background-only hypothesis, respectively. The likelihoods are calculated with the peak position fixed to the known mass of B_c^+ meson [5, 9] and the mass resolution fixed to $10.1\,\mathrm{MeV}/c^2$ as expected from simulation. The statistical significance of the $B_c^+ \to J/\psi\, 3\pi^+ 2\pi^-$ signal is 4.5 standard deviations.

For the selected B_c^+ candidates, the existence of resonant structures is searched for in the $\pi^+\pi^-$, $\pi^+\pi^+\pi^-$, $\pi^+\pi^-\pi^-$, $2\pi^+2\pi^-$, $3\pi^+2\pi^-$ and $J/\psi\,\pi^+\pi^-$ combinations of final state particles using the *sPlot* technique [35], with the reconstructed $J/\psi\, 3\pi^+ 2\pi^-$ mass as discriminating variable, to subtract the background. No significant narrow structures are observed; in particular, no indication of a contribution from $B_c^+ \to \psi(2S)\pi^+\pi^+\pi^-$, followed by the $\psi(2S) \to J/\psi\,\pi^+\pi^-$ decay, is seen. The background-subtracted five-pion mass distribution is shown in figure 2, along with the theoretical prediction in ref. [14], which describes the data well. The consistency between data and the model prediction is estimated using a χ^2-test and gives a p-value of $14\,\%$. The corresponding p-value for the phase space decay model is $4\,\%$.

Parameter		Value
$m_{B_c^+}$	$\left[\,\mathrm{MeV}/c^2\,\right]$	6273 ± 3
$\sigma_{B_c^+}$	$\left[\,\mathrm{MeV}/c^2\,\right]$	11.4 ± 3.4
$N_{B_c^+ \to J/\psi\,3\pi^+2\pi^-}$		32 ± 8

Table 1. Signal parameters of the unbinned extended maximum likelihood fit to the J/$\psi\,3\pi^+2\pi^-$ mass distribution. Uncertainties are statistical only.
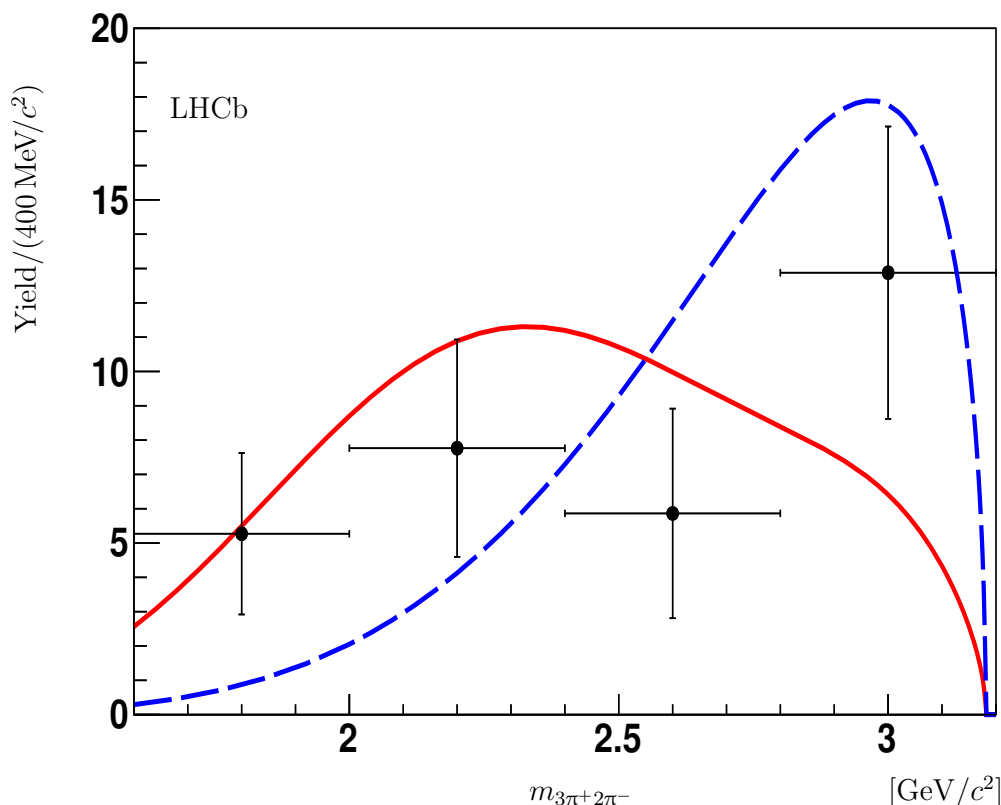

Figure 2. Background-subtracted distribution of five-pion mass from $B_c^+ \to J/\psi\,3\pi^+2\pi^-$ events (points with error bars). The model prediction from ref. [14] is shown by a red solid line, and the expectation from the phase space model is shown by a blue dashed line.

The mass distribution of the selected $B_c^+ \to J/\psi\,\pi^+$ candidates is shown in figure 3, together with the result of an extended unbinned maximum likelihood fit. The B_c^+ signal is modelled by a Gaussian distribution and the background by an exponential function. The fit gives a yield of 2271 ± 63 events.

5   Efficiency and systematic uncertainties

The overall efficiency for each decay is the product of the geometrical acceptance of the detector, reconstruction, selection and trigger efficiencies. These are estimated using simula-
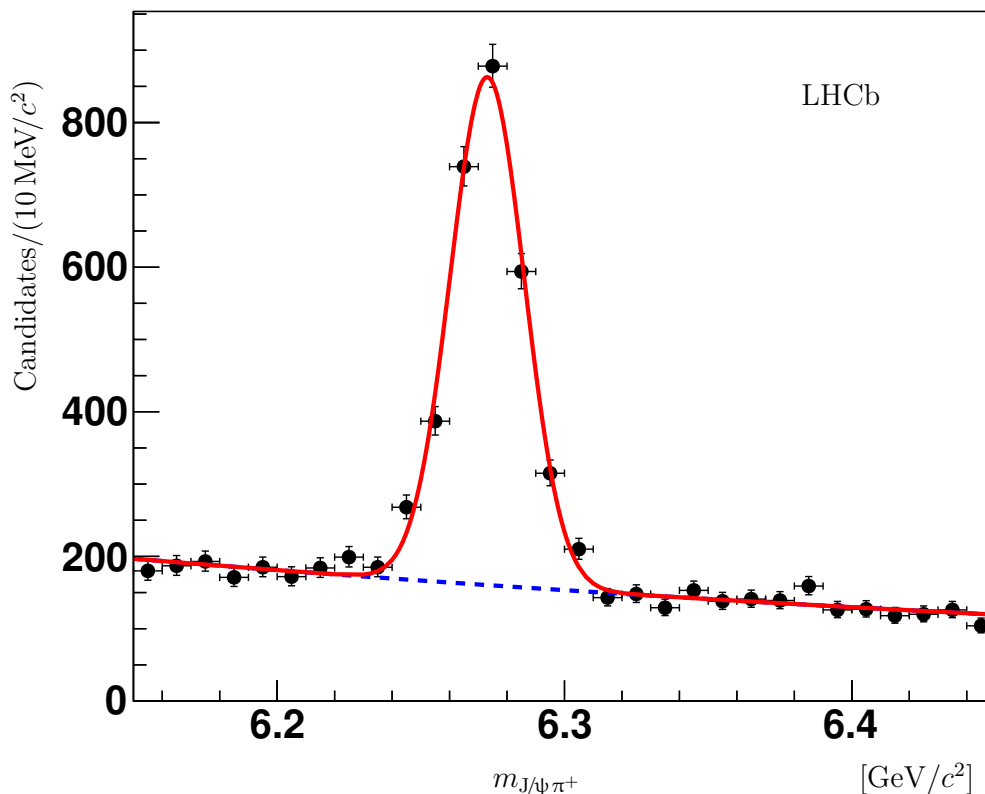
Figure 3. Mass distribution for selected $B_c^+ \to J/\psi \pi^+$ candidates. The result of a fit using the model described in the text (red solid line) is shown together with the background component (blue dashed line).

tion and the ratio of the efficiencies is found to be

$$\frac{\varepsilon(B_c^+ \to J/\psi \pi^+)}{\varepsilon(B_c^+ \to J/\psi 3\pi^+ 2\pi^-)} = 123.8 \pm 5.6 \pm 15.1, \tag{5.1}$$

where the first uncertainty is statistical, due to the finite size of the simulated sample, and the second one is systematic, as discussed below. The large difference in efficiencies is due to the reconstruction of four additional low-p_T pions in the $B_c^+ \to J/\psi 3\pi^+ 2\pi^-$ mode. The efficiencies for the data samples collected at a centre-of-mass energy of 7 TeV and 8 TeV are found to be similar and a luminosity-weighted average is used, with the corresponding systematic uncertainty discussed below.

Many sources of systematic uncertainty cancel in the ratio, in particular those related to the muon and J/ψ reconstruction and identification. Those that do not cancel are discussed below and summarized in table 2.

A systematic uncertainty arises from the imperfect knowledge of the shape of the signal and background in the $J/\psi 3\pi^+ 2\pi^-$ and $J/\psi \pi^+$ mass distributions. The dependence of the signal yields on the fit model is studied by varying the signal and background parameterizations. This is assessed by using Crystal Ball [36] and double-sided Crystal Ball [37] functions for the parameterization of the B_c^+ signals. The background parametrization

Source	Uncertainty [%]
Fit model	6.6
Decay model	
$\quad m_{3\pi^+2\pi^-}$ reweighting	7.7
$\quad \psi(2S)$ mass veto	3.1
Data-simulation agreement	
$\quad$ Hadron interactions	4×2.0
$\quad$ Track quality selection	4×0.6
$\quad$ Trigger	1.1
$\quad$ Pion identification	0.7
$\quad$ Selection variables	1.0
B_c^+ lifetime	0.9
Stability for various data taking conditions	2.5
Acceptance	0.8
Total	13.9

Table 2. Relative systematic uncertainties for the ratio $R_{5\pi}$. The total uncertainty is the quadratic sum of the individual components.

is performed using both exponential and polynomial functions. The maximum observed change of 6.6 % in the ratio of $B_c^+ \to J/\psi\, 3\pi^+2\pi^-$ and $B_c^+ \to J/\psi\, \pi^+$ yields is assigned as a systematic uncertainty.

To assess the systematic uncertainty related to the $B_c^+ \to J/\psi\, 3\pi^+2\pi^-$ decay model used in the simulation [14], the reconstructed mass distribution of the five-pion system in simulated events is reweighted to reproduce the distribution observed in data. As a cross-check the efficiency is also recalculated using a phase space model for the $B_c^+ \to J/\psi\, 3\pi^+2\pi^-$ decays. There is a maximal change in efficiency of 7.7 %, which is taken as the systematic uncertainty for the decay model. In addition, the analysis is repeated with the removal of all B_c^+ candidates where the $J/\psi\, \pi^+\pi^-$ mass is compatible with originating from $\psi(2S) \to J/\psi\, \pi^+\pi^-$ decays. The observed difference of 3.1 % is assigned as an additional systematic uncertainty.

A large class of uncertainties arises from the differences between data and simulation, in particular those affecting the efficiency for reconstruction of charged-particle tracks. The largest of these arises from the simulation of hadronic interactions in the detector, which has an uncertainty of 2 % per track [31, 38, 39]. An additional uncertainty associated with the track quality requirements for the additional four pions in the signal decay is estimated to be 0.6 % per track [5, 7]. The trigger efficiency for events with $J/\psi \to \mu^+\mu^-$ produced in beauty hadron decays is studied on data in high-yield modes [5, 40] and a systematic uncertainty of 1.1 % is assigned based on the comparison of the ratio of trigger efficiencies for high-yield samples of $B^+ \to J/\psi\, K^+$ and $B^+ \to \psi(2S)K^+$ decays on data and simulation [40].

The systematic uncertainty associated with pion identification is studied using a sample of $B^+ \to J/\psi K^+ \pi^+ \pi^-$ decays. The efficiency to identify a $\pi^+\pi^-$ pair is compared for data and simulation. This comparison shows a 0.35% difference between the data and simulation in the efficiency to identify a pion pair. As a result of this study an uncertainty of 0.7% is assigned for the four additional pions in the analysis.

The transverse momentum and rapidity spectra for the selected $B_c^+ \to J/\psi \pi^+$ candidates, as well their daughter J/ψ mesons and pions, are found to be in good agreement with the predictions from the BCVEGPY generator. Good agreement in efficiencies determined from the data and simulation has been observed for all variables used in the selection of $B_c^+ \to J/\psi \pi^+$ candidates. The differences do not exceed 1%, which is used as a conservative estimate for the systematic uncertainty from the selection variables. The agreement between data and simulation has also been cross-checked using the $B_c^+ \to J/\psi 3\pi^+ 2\pi^-$ signal by varying the selection criteria to the values that correspond to a 20% change in the signal yield in simulation. No unexpectedly large deviation is found.

The different acceptance as a function of decay time for the $B_c^+ \to J/\psi 3\pi^+ 2\pi^-$ and $B_c^+ \to J/\psi \pi^+$ decay modes results in an additional systematic uncertainty related to the imprecise knowledge of the B_c^+ lifetime. To assess the related uncertainty, the decay time distributions for simulated events are reweighted after changing the B_c^+ lifetime by one standard deviation around the value of $509 \pm 8 \pm 12$ fs [10] measured by LHCb and the efficiencies are recomputed. The observed 0.9% variation in the ratio of efficiencies is used as the systematic uncertainty.

The uncertainty related to the stability of the analysis results against variations of the detector and trigger configurations occuring in different data-taking periods are tested by studying the ratio of the yields of $B^+ \to J/\psi K^+ \pi^+ \pi^-$ and $B^+ \to J/\psi K^+$ decays as a function of the data-taking period. According to this study an additional systematic uncertainty of 2.5% is assigned [5].

The last systematic uncertainty originates from the dependence of the geometrical acceptance on both the beam crossing angle and the position of the luminosity region. The resulting 0.8% difference in the efficiency ratios is taken as an estimate of the systematic uncertainty.

A summary of systematic uncertainties is presented in table 2. The total systematic uncertainty on the ratio of the branching fractions $R_{5\pi}$ is 13.9%.

6   Results and summary

The first evidence for the decay $B_c^+ \to J/\psi 3\pi^+ 2\pi^-$ is found using pp collisions, corresponding to an integrated luminosity of 3 fb^{-1}, collected with the LHCb detector A signal yield of 32 ± 8 events is found. The significance, taking into account the systematic uncertainties due to the fit function, peak position and mass resolution in the fit, is estimated to be 4.5 standard deviations.

Using the $B_c^+ \to J/\psi \pi^+$ mode as a normalization channel, the ratio of branching fractions is calculated as

$$R_{5\pi} = \frac{N\left(B_c^+ \to J/\psi 3\pi^+ 2\pi^-\right)}{N\left(B_c^+ \to J/\psi \pi^+\right)} \times \frac{\varepsilon(B_c^+ \to J/\psi \pi^+)}{\varepsilon(B_c^+ \to J/\psi 3\pi^+ 2\pi^-)}, \tag{6.1}$$

where N is the number of reconstructed decays obtained from the fit described in section 4 and the efficiency ratio is taken from eq. (5.1). The ratio of branching fractions is measured to be

$$\frac{\mathcal{B}\left(B_c^+ \to J/\psi\, 3\pi^+ 2\pi^-\right)}{\mathcal{B}\left(B_c^+ \to J/\psi\, \pi^+\right)} = 1.74 \pm 0.44 \pm 0.24,$$

where the first uncertainty is statistical and the second is systematic. The result is in agreement with theoretical predictions [14] of 0.95 and 1.1 using the form factors from refs. [15] and [16], respectively. This result is also consistent with analogous measurements in B^0 and B^+ meson decays [9]

$$\frac{\mathcal{B}\left(B^0 \to D^{*-} 3\pi^+ 2\pi^-\right)}{\mathcal{B}\left(B^0 \to D^{*-} \pi^+\right)} = 1.70 \pm 0.34,$$

$$\frac{\mathcal{B}\left(B^+ \to \bar{D}^{*0} 3\pi^+ 2\pi^-\right)}{\mathcal{B}\left(B^+ \to \bar{D}^{*0} \pi^+\right)} = 1.10 \pm 0.24,$$

as expected from factorization.

Acknowledgments

References

[1] CDF collaboration, F. Abe et al., *Observation of the B_c meson in $p\bar{p}$ collisions at $\sqrt{s} = 1.8$ TeV*, *Phys. Rev. Lett.* **81** (1998) 2432 [hep-ex/9805034] [INSPIRE].

[2] CDF collaboration, T. Aaltonen et al., *Observation of the Decay $B_c^+ \to J/\psi\pi^\pm$ and Measurement of the B_c^+ Mass*, *Phys. Rev. Lett.* **100** (2008) 182002 [`arXiv:0712.1506`] [INSPIRE].

[3] LHCb collaboration, *First observation of the decay $B_c^+ \to J/\psi\pi^+\pi^-\pi^+$*, *Phys. Rev. Lett.* **108** (2012) 251802 [`arXiv:1204.0079`] [INSPIRE].

[4] LHCb collaboration, *Observation of the decay $B_c^+ \to \psi(2S)\pi^+$*, *Phys. Rev.* **D 87** (2013) 071103 [`arXiv:1303.1737`] [INSPIRE].

[5] LHCb collaboration, *Observation of $B_c^+ \to J/\psi D_s^+$ and $B_c^+ \to J/\psi D_s^{*+}$ decays*, *Phys. Rev.* **D 87** (2013) 112012 [`arXiv:1304.4530`] [INSPIRE].

[6] LHCb collaboration, *First observation of the decay $B_c^+ \to J/\psi K^+$*, *JHEP* **09** (2013) 075 [`arXiv:1306.6723`] [INSPIRE].

[7] LHCb collaboration, *Observation of the decay $B_c^+ \to J/\psi K^+ K^- \pi^+$*, *JHEP* **11** (2013) 094 [`arXiv:1309.0587`] [INSPIRE].

[8] LHCb collaboration, *Observation of the decay $B_c^+ \to B_s^0\pi^+$*, *Phys. Rev. Lett.* **111** (2013) 181801 [`arXiv:1308.4544`] [INSPIRE].

[9] PARTICLE DATA GROUP collaboration, J. Beringer et al., *Review of particle physics*, *Phys. Rev.* **D 86** (2012) 010001 [INSPIRE].

[10] LHCb collaboration, *Measurement of the B_c^+ meson lifetime using $B_c^+ \to J/\psi\mu^+\nu_\mu X$ decays*, `arXiv:1401.6932` [INSPIRE].

[11] M. Bauer, B. Stech and M. Wirbel, *Exclusive nonleptonic decays of D-, D_s- and B-mesons*, *Z. Phys.* **C 34** (1987) 103 [INSPIRE].

[12] M. Wirbel, *Description of weak decays of D and B Mesons*, *Prog. Part. Nucl. Phys.* **21** (1988) 33 [INSPIRE].

[13] A. Likhoded and A. Luchinsky, *Light hadron production in $B_c \to J/\psi + X$ decays*, *Phys. Rev.* **D 81** (2010) 014015 [`arXiv:0910.3089`] [INSPIRE].

[14] A. Luchinsky, *Production of charged π-mesons in exclusive $B_c \to V(P) + n\pi$ decays*, *Phys. Rev.* **D 86** (2012) 074024 [`arXiv:1208.1398`] [INSPIRE].

[15] V. Kiselev, A. Kovalsky and A. Likhoded, *B_c decays and lifetime in QCD sum rules*, *Nucl. Phys.* **B 585** (2000) 353 [`hep-ph/0002127`] [INSPIRE].

[16] D. Ebert, R. Faustov and V. Galkin, *Weak decays of the B_c meson to charmonium and D mesons in the relativistic quark model*, *Phys. Rev.* **D 68** (2003) 094020 [`hep-ph/0306306`] [INSPIRE].

[17] LHCb collaboration, *The LHCb Detector at the LHC*, 2008 *JINST* **3** S08005 [INSPIRE].

[18] R. Arink et al., *Performance of the LHCb Outer Tracker*, 2014 *JINST* **9** 01002 [`arXiv:1311.3893`] [INSPIRE].

[19] M. Adinolfi et al., *Performance of the LHCb RICH detector at the LHC*, *Eur. Phys. J.* **C 73** (2013) 2431 [`arXiv:1211.6759`] [INSPIRE].

[20] J. Alves et al., *Performance of the LHCb muon system*, 2013 *JINST* **8** P02022 [`arXiv:1211.1346`] [INSPIRE].

[21] R. Aaij et al., *The LHCb trigger and its performance in 2011*, 2013 *JINST* **8** P04022 [`arXiv:1211.3055`] [INSPIRE].

[22] T. Sjöstrand, S. Mrenna and P.Z. Skands, *PYTHIA 6.4 physics and manual*, *JHEP* **05** (2006) 026 [hep-ph/0603175] [INSPIRE].

[23] I. Belyaev et al., *Handling of the generation of primary events in* GAUSS, *the LHCb simulation framework*, *IEEE Nucl. Sci. Symp. Conf. Rec.* **IEEE** (2010) 1155.

[24] P. Golonka and Z. Was, *PHOTOS Monte Carlo: a precision tool for QED corrections in Z and W decays*, *Eur. Phys. J.* **C 45** (2006) 97 [hep-ph/0506026] [INSPIRE].

[25] C.-H. Chang, C. Driouichi, P. Eerola and X.G. Wu, *BCVEGPY: an event generator for hadronic production of the B_c meson*, *Comput. Phys. Commun.* **159** (2004) 192 [hep-ph/0309120] [INSPIRE].

[26] D. Lange, *The EvtGen particle decay simulation package*, *Nucl. Instrum. Meth.* **A 462** (2001) 152 [INSPIRE].

[27] BABAR collaboration, J. Lees et al., *Study of high-multiplicity 3-prong and 5-prong τ decays at BABAR*, *Phys. Rev.* **D 86** (2012) 092010 [arXiv:1209.2734] [INSPIRE].

[28] GEANT4 collaboration, J. Allison et al., *GEANT4 developments and applications*, *IEEE Trans. Nucl. Sci.* **53** (2006) 270.

[29] GEANT4 collaboration, S. Agostinelli et al., *GEANT4 — a simulation toolkit*, *Nucl. Instrum. Meth.* **A 506** (2003) 250 [INSPIRE].

[30] M. Clemencic et al., *The LHCb simulation application, Gauss: design, evolution and experience*, *J. Phys. Conf. Ser.* **331** (2011) 032023 [INSPIRE].

[31] R. Aaij et al., *Measurement of the track reconstruction efficiency at LHCb*, LHCb-DP-2013-002, in preparation.

[32] F. Archilli et al., *Performance of the muon identification at LHCb*, 2013 *JINST* **8** P10020 [arXiv:1306.0249] [INSPIRE].

[33] R. Aaij et al., *Performance of the LHCb calorimeters*, LHCb-DP-2013-004, in preparation.

[34] W.D. Hulsbergen, *Decay chain fitting with a Kalman filter*, *Nucl. Instrum. Meth.* **A 552** (2005) 566 [physics/0503191] [INSPIRE].

[35] M. Pivk and F.R. Le Diberder, *SPlot: a statistical tool to unfold data distributions*, *Nucl. Instrum. Meth.* **A 555** (2005) 356 [physics/0402083] [INSPIRE].

[36] T. Skwarnicki, *A study of the radiative cascade transitions between the Υ' and Υ resonances*, Ph.D. thesis, Institute of Nuclear Physics, Krakow, Poland (1986), DESY-F31-86-02 [INSPIRE].

[37] LHCb collaboration, *Observation of J/ψ pair production in pp collisions at $\sqrt{s} = 7TeV$*, *Phys. Lett.* **B 707** (2012) 52 [arXiv:1109.0963] [INSPIRE].

[38] A. Jaeger et al., *Measurement of the track finding efficiency*, LHCb-PUB-2011-025 (2011).

[39] LHCb collaboration, *Prompt K_s^0 production in pp collisions at $\sqrt{s} = 0.9$ TeV*, *Phys. Lett.* **B 693** (2010) 69 [arXiv:1008.3105] [INSPIRE].

[40] LHCb collaboration, *Measurement of relative branching fractions of B decays to $\psi(2S)$ and J/ψ mesons*, *Eur. Phys. J.* **C 72** (2012) 2118 [arXiv:1205.0918] [INSPIRE].

The LHCb collaboration

R. Aaij[41], B. Adeva[37], M. Adinolfi[46], A. Affolder[52], Z. Ajaltouni[5], J. Albrecht[9], F. Alessio[38],
M. Alexander[51], S. Ali[41], G. Alkhazov[30], P. Alvarez Cartelle[37], A.A. Alves Jr[25,38], S. Amato[2],
S. Amerio[22], Y. Amhis[7], L. An[3], L. Anderlini[17,g], J. Anderson[40], R. Andreassen[57],
M. Andreotti[16,f], J.E. Andrews[58], R.B. Appleby[54], O. Aquines Gutierrez[10], F. Archilli[38],
A. Artamonov[35], M. Artuso[59], E. Aslanides[6], G. Auriemma[25,m], M. Baalouch[5], S. Bachmann[11],
J.J. Back[48], A. Badalov[36], V. Balagura[31], W. Baldini[16], R.J. Barlow[54], C. Barschel[38], S. Barsuk[7],
W. Barter[47], V. Batozskaya[28], Th. Bauer[41], A. Bay[39], J. Beddow[51], F. Bedeschi[23], I. Bediaga[1],
S. Belogurov[31], K. Belous[35], I. Belyaev[31], E. Ben-Haim[8], G. Bencivenni[18], S. Benson[50],
J. Benton[46], A. Berezhnoy[32], R. Bernet[40], M.-O. Bettler[47], M. van Beuzekom[41], A. Bien[11],
S. Bifani[45], T. Bird[54], A. Bizzeti[17,i], P.M. Bjørnstad[54], T. Blake[48], F. Blanc[39], J. Blouw[10],
S. Blusk[59], V. Bocci[25], A. Bondar[34], N. Bondar[30,38], W. Bonivento[15,38], S. Borghi[54], A. Borgia[59],
M. Borsato[7], T.J.V. Bowcock[52], E. Bowen[40], C. Bozzi[16], T. Brambach[9], J. van den Brand[42],
J. Bressieux[39], D. Brett[54], M. Britsch[10], T. Britton[59], N.H. Brook[46], H. Brown[52], A. Bursche[40],
G. Busetto[22,p], J. Buytaert[38], S. Cadeddu[15], R. Calabrese[16,f], O. Callot[7], M. Calvi[20,k],
M. Calvo Gomez[36,n], A. Camboni[36], P. Campana[18,38], D. Campora Perez[38], F. Caponio[21,t],
A. Carbone[14,d], G. Carboni[24,l], R. Cardinale[19,38,j], A. Cardini[15], H. Carranza-Mejia[50],
L. Carson[50], K. Carvalho Akiba[2], G. Casse[52], L. Cassina[20], L. Castillo Garcia[38], M. Cattaneo[38],
Ch. Cauet[9], R. Cenci[58], M. Charles[8], Ph. Charpentier[38], S.-F. Cheung[55], N. Chiapolini[40],
M. Chrzaszcz[40,26], K. Ciba[38], X. Cid Vidal[38], G. Ciezarek[53], P.E.L. Clarke[50], M. Clemencic[38],
H.V. Cliff[47], J. Closier[38], C. Coca[29], V. Coco[38], J. Cogan[6], E. Cogneras[5], P. Collins[38],
A. Comerma-Montells[11], A. Contu[15,38], A. Cook[46], M. Coombes[46], S. Coquereau[8], G. Corti[38],
I. Counts[56], B. Couturier[38], G.A. Cowan[50], D.C. Craik[48], M. Cruz Torres[60], S. Cunliffe[53],
R. Currie[50], C. D'Ambrosio[38], J. Dalseno[46], P. David[8], P.N.Y. David[41], A. Davis[57],
K. De Bruyn[41], S. De Capua[54], M. De Cian[11], J.M. De Miranda[1], L. De Paula[2], W. De Silva[57],
P. De Simone[18], D. Decamp[4], M. Deckenhoff[9], L. Del Buono[8], N. Déléage[4], D. Derkach[55],
O. Deschamps[5], F. Dettori[42], A. Di Canto[38], H. Dijkstra[38], S. Donleavy[52], F. Dordei[11],
M. Dorigo[39], A. Dosil Suárez[37], D. Dossett[48], A. Dovbnya[43], F. Dupertuis[39], P. Durante[38],
R. Dzhelyadin[35], A. Dziurda[26], A. Dzyuba[30], S. Easo[49], U. Egede[53], V. Egorychev[31],
S. Eidelman[34], S. Eisenhardt[50], U. Eitschberger[9], R. Ekelhof[9], L. Eklund[51,38], I. El Rifai[5],
Ch. Elsasser[40], S. Esen[11], A. Falabella[16,f], C. Färber[11], C. Farinelli[41], N. Farley[45], S. Farry[52],
D. Ferguson[50], V. Fernandez Albor[37], F. Ferreira Rodrigues[1], M. Ferro-Luzzi[38], S. Filippov[33],
M. Fiore[16,f], M. Fiorini[16,f], M. Firlej[27], C. Fitzpatrick[38], T. Fiutowski[27], M. Fontana[10],
F. Fontanelli[19,j], R. Forty[38], O. Francisco[2], M. Frank[38], C. Frei[38], M. Frosini[17,38,g], J. Fu[21],
E. Furfaro[24,l], A. Gallas Torreira[37], D. Galli[14,d], S. Gallorini[22], S. Gambetta[19,j], M. Gandelman[2],
P. Gandini[59], Y. Gao[3], J. Garofoli[59], J. Garra Tico[47], L. Garrido[36], C. Gaspar[38], R. Gauld[55],
L. Gavardi[9], E. Gersabeck[11], M. Gersabeck[54], T. Gershon[48], Ph. Ghez[4], A. Gianelle[22],
S. Giani'[39], V. Gibson[47], L. Giubega[29], V.V. Gligorov[38], C. Göbel[60], D. Golubkov[31],
A. Golutvin[53,31,38], A. Gomes[1,a], H. Gordon[38], C. Gotti[20], M. Grabalosa Gándara[5],
R. Graciani Diaz[36], L.A. Granado Cardoso[38], E. Graugés[36], G. Graziani[17], A. Grecu[29],
E. Greening[55], S. Gregson[47], P. Griffith[45], L. Grillo[11], O. Grünberg[62], B. Gui[59], E. Gushchin[33],
Yu. Guz[35,38], T. Gys[38], C. Hadjivasiliou[59], G. Haefeli[39], C. Haen[38], T.W. Hafkenscheid[65],
S.C. Haines[47], S. Hall[53], B. Hamilton[58], T. Hampson[46], X. Han[11], S. Hansmann-Menzemer[11],
N. Harnew[55], S.T. Harnew[46], J. Harrison[54], T. Hartmann[62], J. He[38], T. Head[38], V. Heijne[41],
K. Hennessy[52], P. Henrard[5], L. Henry[8], J.A. Hernando Morata[37], E. van Herwijnen[38], M. Heß[62],
A. Hicheur[1], D. Hill[55], M. Hoballah[5], C. Hombach[54], W. Hulsbergen[41], P. Hunt[55], N. Hussain[55],
D. Hutchcroft[52], D. Hynds[51], M. Idzik[27], P. Ilten[56], R. Jacobsson[38], A. Jaeger[11], E. Jans[41],

P. Jaton[39], A. Jawahery[58], M. Jezabek[26], F. Jing[3], M. John[55], D. Johnson[55], C.R. Jones[47],
C. Joram[38], B. Jost[38], N. Jurik[59], M. Kaballo[9], S. Kandybei[43], W. Kanso[6], M. Karacson[38],
T.M. Karbach[38], M. Kelsey[59], I.R. Kenyon[45], T. Ketel[42], B. Khanji[20], C. Khurewathanakul[39],
S. Klaver[54], O. Kochebina[7], M. Kolpin[11], I. Komarov[39], R.F. Koopman[42], P. Koppenburg[41,38],
M. Korolev[32], A. Kozlinskiy[41], L. Kravchuk[33], K. Kreplin[11], M. Kreps[48], G. Krocker[11],
P. Krokovny[34], F. Kruse[9], M. Kucharczyk[20,26,38,k], V. Kudryavtsev[34], K. Kurek[28],
T. Kvaratskheliya[31], V.N. La Thi[39], D. Lacarrere[38], G. Lafferty[54], A. Lai[15], D. Lambert[50],
R.W. Lambert[42], E. Lanciotti[38], G. Lanfranchi[18], C. Langenbruch[38], B. Langhans[38],
T. Latham[48], C. Lazzeroni[45], R. Le Gac[6], J. van Leerdam[41], J.-P. Lees[4], R. Lefèvre[5], A. Leflat[32],
J. Lefrançois[7], S. Leo[23], O. Leroy[6], T. Lesiak[26], B. Leverington[11], Y. Li[3], M. Liles[52],
R. Lindner[38], C. Linn[38], F. Lionetto[40], B. Liu[15], G. Liu[38], S. Lohn[38], I. Longstaff[51], J.H. Lopes[2],
N. Lopez-March[39], P. Lowdon[40], H. Lu[3], D. Lucchesi[22,p], H. Luo[50], E. Luppi[16,f], O. Lupton[55],
F. Machefert[7], I.V. Machikhiliyan[31], F. Maciuc[29], O. Maev[30], S. Malde[55], G. Manca[15,e],
G. Mancinelli[6], M. Manzali[16,f], J. Maratas[5], J.F. Marchand[4], U. Marconi[14], C. Marin Benito[36],
P. Marino[23,r], R. Märki[39], J. Marks[11], G. Martellotti[25], A. Martens[8], A. Martín Sánchez[7],
M. Martinelli[41], D. Martinez Santos[42], F. Martinez Vidal[64], D. Martins Tostes[2], A. Massafferri[1],
R. Matev[38], Z. Mathe[38], C. Matteuzzi[20], A. Mazurov[16,f], M. McCann[53], J. McCarthy[45],
A. McNab[54], R. McNulty[12], B. McSkelly[52], B. Meadows[57,55], F. Meier[9], M. Meissner[11],
M. Merk[41], D.A. Milanes[8], M.-N. Minard[4], J. Molina Rodriguez[60], S. Monteil[5], D. Moran[54],
M. Morandin[22], P. Morawski[26], A. Mordà[6], M.J. Morello[23,r], J. Moron[27], R. Mountain[59],
F. Muheim[50], K. Müller[40], R. Muresan[29], B. Muster[39], P. Naik[46], T. Nakada[39],
R. Nandakumar[49], I. Nasteva[2], M. Needham[50], N. Neri[21], S. Neubert[38], N. Neufeld[38],
M. Neuner[11], A.D. Nguyen[39], T.D. Nguyen[39], C. Nguyen-Mau[39,o], M. Nicol[7], V. Niess[5], R. Niet[9],
N. Nikitin[32], T. Nikodem[11], A. Novoselov[35], A. Oblakowska-Mucha[27], V. Obraztsov[35],
S. Oggero[41], S. Ogilvy[51], O. Okhrimenko[44], R. Oldeman[15,e], G. Onderwater[65], M. Orlandea[29],
J.M. Otalora Goicochea[2], P. Owen[53], A. Oyanguren[36], B.K. Pal[59], A. Palano[13,c], F. Palombo[21,s],
M. Palutan[18], J. Panman[38], A. Papanestis[49,38], M. Pappagallo[51], L. Pappalardo[16], C. Parkes[54],
C.J. Parkinson[9], G. Passaleva[17], G.D. Patel[52], M. Patel[53], C. Patrignani[19,j], A. Pazos Alvarez[37],
A. Pearce[54], A. Pellegrino[41], M. Pepe Altarelli[38], S. Perazzini[14,d], E. Perez Trigo[37], P. Perret[5],
M. Perrin-Terrin[6], L. Pescatore[45], E. Pesen[66], K. Petridis[53], A. Petrolini[19,j],
E. Picatoste Olloqui[36], B. Pietrzyk[4], T. Pilař[48], D. Pinci[25], A. Pistone[19], S. Playfer[50],
M. Plo Casasus[37], F. Polci[8], A. Poluektov[48,34], E. Polycarpo[2], A. Popov[35], D. Popov[10],
B. Popovici[29], C. Potterat[2], A. Powell[55], J. Prisciandaro[39], A. Pritchard[52], C. Prouve[46],
V. Pugatch[44], A. Puig Navarro[39], G. Punzi[23,q], W. Qian[4], B. Rachwal[26], J.H. Rademacker[46],
B. Rakotomiaramanana[39], M. Rama[18], M.S. Rangel[2], I. Raniuk[43], N. Rauschmayr[38], G. Raven[42],
S. Reichert[54], M.M. Reid[48], A.C. dos Reis[1], S. Ricciardi[49], A. Richards[53], K. Rinnert[52],
V. Rives Molina[36], D.A. Roa Romero[5], P. Robbe[7], D.A. Roberts[58], A.B. Rodrigues[1],
E. Rodrigues[54], P. Rodriguez Perez[54], S. Roiser[38], V. Romanovsky[35], A. Romero Vidal[37],
M. Rotondo[22], J. Rouvinet[39], T. Ruf[38], F. Ruffini[23], H. Ruiz[36], P. Ruiz Valls[36], G. Sabatino[25,l],
J.J. Saborido Silva[37], N. Sagidova[30], P. Sail[51], B. Saitta[15,e], V. Salustino Guimaraes[2],
B. Sanmartin Sedes[37], R. Santacesaria[25], C. Santamarina Rios[37], E. Santovetti[24,l], M. Sapunov[6],
A. Sarti[18], C. Satriano[25,m], A. Satta[24], M. Savrie[16,f], D. Savrina[31,32], M. Schiller[42],
H. Schindler[38], M. Schlupp[9], M. Schmelling[10], B. Schmidt[38], O. Schneider[39], A. Schopper[38],
M.-H. Schune[7], R. Schwemmer[38], B. Sciascia[18], A. Sciubba[25], M. Seco[37], A. Semennikov[31],
K. Senderowska[27], I. Sepp[53], N. Serra[40], J. Serrano[6], P. Seyfert[11], M. Shapkin[35],
I. Shapoval[16,43,f], Y. Shcheglov[30], T. Shears[52], L. Shekhtman[34], O. Shevchenko[43],
V. Shevchenko[63], A. Shires[9], F. Sidorov[31], R. Silva Coutinho[48], G. Simi[22], M. Sirendi[47],
N. Skidmore[46], T. Skwarnicki[59], N.A. Smith[52], E. Smith[55,49], E. Smith[53], J. Smith[47], M. Smith[54],

H. Snoek[41], M.D. Sokoloff[57], F.J.P. Soler[51], F. Soomro[39], D. Souza[46], B. Souza De Paula[2],
B. Spaan[9], A. Sparkes[50], F. Spinella[23], P. Spradlin[51], F. Stagni[38], S. Stahl[11], O. Steinkamp[40],
S. Stevenson[55], S. Stoica[29], S. Stone[59], B. Storaci[40], S. Stracka[23,38], M. Straticiuc[29],
U. Straumann[40], R. Stroili[22], V.K. Subbiah[38], L. Sun[57], W. Sutcliffe[53], K. Swientek[27],
S. Swientek[9], V. Syropoulos[42], M. Szczekowski[28], P. Szczypka[39,38], D. Szilard[2], T. Szumlak[27],
S. T'Jampens[4], M. Teklishyn[7], G. Tellarini[16,f], F. Teubert[38], C. Thomas[55], E. Thomas[38],
J. van Tilburg[41], V. Tisserand[4], M. Tobin[39], S. Tolk[42], L. Tomassetti[16,f], D. Tonelli[38],
S. Topp-Joergensen[55], N. Torr[55], E. Tournefier[4], S. Tourneur[39], M.T. Tran[39], M. Tresch[40],
A. Tsaregorodtsev[6], P. Tsopelas[41], N. Tuning[41], M. Ubeda Garcia[38], A. Ukleja[28],
A. Ustyuzhanin[63], U. Uwer[11], V. Vagnoni[14], G. Valenti[14], A. Vallier[7], R. Vazquez Gomez[18],
P. Vazquez Regueiro[37], C. Vázquez Sierra[37], S. Vecchi[16], J.J. Velthuis[46], M. Veltri[17,h],
G. Veneziano[39], M. Vesterinen[11], B. Viaud[7], D. Vieira[2], X. Vilasis-Cardona[36,n], A. Vollhardt[40],
D. Volyanskyy[10], D. Voong[46], A. Vorobyev[30], V. Vorobyev[34], C. Voß[62], H. Voss[10], J.A. de Vries[41],
R. Waldi[62], C. Wallace[48], R. Wallace[12], S. Wandernoth[11], J. Wang[59], D.R. Ward[47],
N.K. Watson[45], D. Websdale[53], M. Whitehead[48], J. Wicht[38], D. Wiedner[11], G. Wilkinson[55],
M.P. Williams[48,49], M. Williams[56], F.F. Wilson[49], J. Wimberley[58], J. Wishahi[9], W. Wislicki[28],
M. Witek[26], G. Wormser[7], S.A. Wotton[47], S. Wright[47], S. Wu[3], K. Wyllie[38], Y. Xie[61], Z. Xing[59],
Z. Yang[3], X. Yuan[3], O. Yushchenko[35], M. Zangoli[14], M. Zavertyaev[10,b], F. Zhang[3], L. Zhang[59],
W.C. Zhang[12], Y. Zhang[3], A. Zhelezov[11], A. Zhokhov[31], L. Zhong[3], A. Zvyagin[38]

¹ Centro Brasileiro de Pesquisas Físicas (CBPF), Rio de Janeiro, Brazil
² Universidade Federal do Rio de Janeiro (UFRJ), Rio de Janeiro, Brazil
³ Center for High Energy Physics, Tsinghua University, Beijing, China
⁴ LAPP, Université de Savoie, CNRS/IN2P3, Annecy-Le-Vieux, France
⁵ Clermont Université, Université Blaise Pascal, CNRS/IN2P3, LPC, Clermont-Ferrand, France
⁶ CPPM, Aix-Marseille Université, CNRS/IN2P3, Marseille, France
⁷ LAL, Université Paris-Sud, CNRS/IN2P3, Orsay, France
⁸ LPNHE, Université Pierre et Marie Curie, Université Paris Diderot, CNRS/IN2P3, Paris, France
⁹ Fakultät Physik, Technische Universität Dortmund, Dortmund, Germany
¹⁰ Max-Planck-Institut für Kernphysik (MPIK), Heidelberg, Germany
¹¹ Physikalisches Institut, Ruprecht-Karls-Universität Heidelberg, Heidelberg, Germany
¹² School of Physics, University College Dublin, Dublin, Ireland
¹³ Sezione INFN di Bari, Bari, Italy
¹⁴ Sezione INFN di Bologna, Bologna, Italy
¹⁵ Sezione INFN di Cagliari, Cagliari, Italy
¹⁶ Sezione INFN di Ferrara, Ferrara, Italy
¹⁷ Sezione INFN di Firenze, Firenze, Italy
¹⁸ Laboratori Nazionali dell'INFN di Frascati, Frascati, Italy
¹⁹ Sezione INFN di Genova, Genova, Italy
²⁰ Sezione INFN di Milano Bicocca, Milano, Italy
²¹ Sezione INFN di Milano, Milano, Italy
²² Sezione INFN di Padova, Padova, Italy
²³ Sezione INFN di Pisa, Pisa, Italy
²⁴ Sezione INFN di Roma Tor Vergata, Roma, Italy
²⁵ Sezione INFN di Roma La Sapienza, Roma, Italy
²⁶ Henryk Niewodniczanski Institute of Nuclear Physics Polish Academy of Sciences, Kraków, Poland
²⁷ AGH - University of Science and Technology, Faculty of Physics and Applied Computer Science, Kraków, Poland
²⁸ National Center for Nuclear Research (NCBJ), Warsaw, Poland
²⁹ Horia Hulubei National Institute of Physics and Nuclear Engineering, Bucharest-Magurele, Romania

[30] *Petersburg Nuclear Physics Institute (PNPI), Gatchina, Russia*

[31] *Institute of Theoretical and Experimental Physics (ITEP), Moscow, Russia*

[32] *Institute of Nuclear Physics, Moscow State University (SINP MSU), Moscow, Russia*

[33] *Institute for Nuclear Research of the Russian Academy of Sciences (INR RAN), Moscow, Russia*

[34] *Budker Institute of Nuclear Physics (SB RAS) and Novosibirsk State University, Novosibirsk, Russia*

[35] *Institute for High Energy Physics (IHEP), Protvino, Russia*

[36] *Universitat de Barcelona, Barcelona, Spain*

[37] *Universidad de Santiago de Compostela, Santiago de Compostela, Spain*

[38] *European Organization for Nuclear Research (CERN), Geneva, Switzerland*

[39] *Ecole Polytechnique Fédérale de Lausanne (EPFL), Lausanne, Switzerland*

[40] *Physik-Institut, Universität Zürich, Zürich, Switzerland*

[41] *Nikhef National Institute for Subatomic Physics, Amsterdam, The Netherlands*

[42] *Nikhef National Institute for Subatomic Physics and VU University Amsterdam, Amsterdam, The Netherlands*

[43] *NSC Kharkiv Institute of Physics and Technology (NSC KIPT), Kharkiv, Ukraine*

[44] *Institute for Nuclear Research of the National Academy of Sciences (KINR), Kyiv, Ukraine*

[45] *University of Birmingham, Birmingham, United Kingdom*

[46] *H.H. Wills Physics Laboratory, University of Bristol, Bristol, United Kingdom*

[47] *Cavendish Laboratory, University of Cambridge, Cambridge, United Kingdom*

[48] *Department of Physics, University of Warwick, Coventry, United Kingdom*

[49] *STFC Rutherford Appleton Laboratory, Didcot, United Kingdom*

[50] *School of Physics and Astronomy, University of Edinburgh, Edinburgh, United Kingdom*

[51] *School of Physics and Astronomy, University of Glasgow, Glasgow, United Kingdom*

[52] *Oliver Lodge Laboratory, University of Liverpool, Liverpool, United Kingdom*

[53] *Imperial College London, London, United Kingdom*

[54] *School of Physics and Astronomy, University of Manchester, Manchester, United Kingdom*

[55] *Department of Physics, University of Oxford, Oxford, United Kingdom*

[56] *Massachusetts Institute of Technology, Cambridge, MA, United States*

[57] *University of Cincinnati, Cincinnati, OH, United States*

[58] *University of Maryland, College Park, MD, United States*

[59] *Syracuse University, Syracuse, NY, United States*

[60] *Pontifícia Universidade Católica do Rio de Janeiro (PUC-Rio), Rio de Janeiro, Brazil, associated to [2]*

[61] *Institute of Particle Physics, Central China Normal University, Wuhan, Hubei, China, associated to [3]*

[62] *Institut für Physik, Universität Rostock, Rostock, Germany, associated to [11]*

[63] *National Research Centre Kurchatov Institute, Moscow, Russia, associated to [31]*

[64] *Instituto de Fisica Corpuscular (IFIC), Universitat de Valencia-CSIC, Valencia, Spain, associated to [36]*

[65] *KVI - University of Groningen, Groningen, The Netherlands, associated to [41]*

[66] *Celal Bayar University, Manisa, Turkey, associated to [38]*

[a] *Universidade Federal do Triângulo Mineiro (UFTM), Uberaba-MG, Brazil*

[b] *P.N. Lebedev Physical Institute, Russian Academy of Science (LPI RAS), Moscow, Russia*

[c] *Università di Bari, Bari, Italy*

[d] *Università di Bologna, Bologna, Italy*

[e] *Università di Cagliari, Cagliari, Italy*

[f] *Università di Ferrara, Ferrara, Italy*

[g] *Università di Firenze, Firenze, Italy*

[h] *Università di Urbino, Urbino, Italy*

[i] *Università di Modena e Reggio Emilia, Modena, Italy*

[j] Università di Genova, Genova, Italy

[k] Università di Milano Bicocca, Milano, Italy

[l] Università di Roma Tor Vergata, Roma, Italy

[m] Università della Basilicata, Potenza, Italy

[n] LIFAELS, La Salle, Universitat Ramon Llull, Barcelona, Spain

[o] Hanoi University of Science, Hanoi, Viet Nam

[p] Università di Padova, Padova, Italy

[q] Università di Pisa, Pisa, Italy

[r] Scuola Normale Superiore, Pisa, Italy

[s] Università degli Studi di Milano, Milano, Italy

[t] Politecnico di Milano, Milano, Italy